



Chinese Pharmaceutical Association
Institute of Materia Medica, Chinese Academy of Medical Sciences

Acta Pharmaceutica Sinica B

www.elsevier.com/locate/apsb
www.sciencedirect.com



ORIGINAL ARTICLE

Targeting macrophagic SHP2 for ameliorating osteoarthritis via TLR signaling



Ziying Sun^{a,b,†}, Qianqian Liu^{c,†}, Zhongyang Lv^{a,b}, Jiawei Li^{a,b},
Xingquan Xu^{a,b}, Heng Sun^{a,b}, Maochun Wang^{a,b}, Kuoyang Sun^{a,b},
Tianshu Shi^{a,b}, Zizheng Liu^{a,b}, Guihua Tan^{a,b}, Wenqiang Yan^{a,b},
Rui Wu^{a,b}, Yannick Xiaofan Yang^{a,d}, Shiro Ikegawa^{a,e}, Qing Jiang^{a,b},
Yang Sun^{c,*}, Dongquan Shi^{a,b,*}

^aState Key Laboratory of Pharmaceutical Biotechnology, Department of Sports Medicine and Adult Reconstructive Surgery, Nanjing Drum Tower Hospital, the Affiliated Hospital of Nanjing University Medical School, Nanjing 210008, China

^bLaboratory for Bone and Joint Disease, Model Animal Research Center (MARC), Nanjing University, Nanjing 210093, China

^cState Key Laboratory of Pharmaceutical Biotechnology, Department of Biotechnology and Pharmaceutical Sciences, School of Life Science, Nanjing University, Nanjing 210023, China

^dDrum Tower of Clinical Medicine, Nanjing Medical University, Nanjing 210008, China

^eLaboratory for Bone and Joint Diseases, RIKEN Center for Integrative Medical Science (IMS, RIKEN), Tokyo 108-8639, Japan

Received 17 October 2021; received in revised form 15 December 2021; accepted 20 January 2022

KEY WORDS

SHP2;
SHP099;
Osteoarthritis;
Synovitis;
Toll-like receptor
signaling;
Macrophage;
Cartilage degradation;

Abstract Osteoarthritis (OA), in which M1 macrophage polarization in the synovium exacerbates disease progression, is a major cause of cartilage degeneration and functional disabilities. Therapeutic strategies of OA designed to interfere with the polarization of macrophages have rarely been reported. Here, we report that SHP099, as an allosteric inhibitor of src-homology 2-containing protein tyrosine phosphatase 2 (SHP2), attenuated osteoarthritis progression by inhibiting M1 macrophage polarization. We demonstrated that M1 macrophage polarization was accompanied by the overexpression of SHP2 in the synovial tissues of OA patients and OA model mice. Compared to wild-type (WT) mice, myeloid lineage conditional *Shp2* knockout (cKO) mice showed decreased M1 macrophage polarization and attenuated severity of synovitis, an elevated expression of cartilage phenotype protein collagen II (COL2), and a

*Corresponding authors.

E-mail addresses: shidongquan@nju.edu.cn (Dongquan Shi), yangsun@nju.edu.cn (Yang Sun).

†These authors made equal contributions to this work.

Peer review under responsibility of Chinese Pharmaceutical Association and Institute of Materia Medica, Chinese Academy of Medical Sciences.

<https://doi.org/10.1016/j.apsb.2022.02.010>

2211-3835 © 2022 Chinese Pharmaceutical Association and Institute of Materia Medica, Chinese Academy of Medical Sciences. Production and hosting by Elsevier B.V. This is an open access article under the CC BY-NC-ND license (<http://creativecommons.org/licenses/by-nc-nd/4.0/>).

M1 macrophage polarization

decreased expression of cartilage degradation markers collagen X (COL10) and matrix metalloproteinase 3 (MMP3) in OA cartilage. Further mechanistic analysis showed that SHP099 inhibited lipopolysaccharide (LPS)-induced Toll-like receptor (TLR) signaling mediated by nuclear factor kappa B (NF- κ B) and PI3K–AKT signaling. Moreover, intra-articular injection of SHP099 also significantly attenuated OA progression, including joint synovitis and cartilage damage. These results indicated that allosteric inhibition of SHP2 might be a promising therapeutic strategy for the treatment of OA.

© 2022 Chinese Pharmaceutical Association and Institute of Materia Medica, Chinese Academy of Medical Sciences. Production and hosting by Elsevier B.V. This is an open access article under the CC BY-NC-ND license (<http://creativecommons.org/licenses/by-nc-nd/4.0/>).

1. Introduction

Osteoarthritis (OA) is a senile disease with a high incidence that affects 10% of men and 18% of women over the age of 60 years old¹. OA is characterized by cartilage degeneration, subchondral bone remodelling and synovial inflammation (synovitis)². Synovitis in OA is related to severe pain and joint dysfunction and accelerates cartilage loss³. Histological changes in synovitis include synovial lining hyperplasia, macrophage and lymphocyte infiltration and new blood vessel formation⁴.

Macrophages determine inflammatory marker expression during synovitis⁵ and are divided into two types, namely, M1 and M2 macrophages. M1 macrophages can release inflammatory factors, such as Interleukin (IL)-1 and IL-6, while M2 macrophages can release protective cytokines, such as IL-10⁶. The promotion of M1 macrophage polarization can aggravate OA progression⁷. However, conditional macrophage deletion has no significant impact on the development of OA⁸. Intervention for macrophage M1 polarization to attenuate the severity of OA is awaited to be investigated.

Src-homology 2-containing protein tyrosine phosphatase 2 (SHP2) is a widely expressed non-receptor protein tyrosine phosphatase⁹. SHP2 plays an essential role in organism development and physiological and pathological reactions in response to growth and stimulatory factors^{10,11}. It inhibited NOD-like receptor protein 3 (NLRP3) inflammasome activation in macrophages¹². However, a recent study demonstrated that SHP2 exacerbated inflammation by inhibiting macrophage responsiveness to IL-10¹³. Our previous research revealed that SHP2 exacerbated the imbalance between cartilage catabolism and anabolism by regulating the DOK1–UPP1–uridine axis and promoted the progression of osteoarthritis¹⁴, but it is still unclear whether SHP2 affects immune cells in the joint microenvironment, especially macrophages, to regulate the progression of OA. SHP099 is a potent (IC₅₀ = 71 nmol/L) and selective allosteric inhibitor of SHP2, which concurrently binds to the interface of the protein tyrosine phosphatase domains, N-terminal SH2 and C-terminal SH2, thus inhibiting SHP2 activity through an allosteric mechanism¹⁵. The research on SHP099 focuses on its ability in inhibiting cancer cell growth and enhancing anti-tumor immunity¹⁶. Exploring the role of SHP2 in macrophage polarization during the progression of OA and the potential application of its allosteric inhibitor would provide a new strategy for treating OA.

In this study, we found that SHP2 was highly expressed in OA synovial macrophages. Conditional *Shp2* knockout (cKO) mice exhibited decreased M1 macrophage polarization and less cartilage degeneration in the destabilization of medial meniscus (DMM) model, a surgically induced OA mouse model¹⁷. SHP099, a SHP2 allosteric inhibitor, attenuated lipopolysaccharide (LPS)-

induced M1 macrophage inflammation in bone marrow-derived macrophages (BMDMs) and RAW264.7 cells and inhibited M1 polarization of macrophages by suppressing LPS-induced Toll-like receptor (TLR) signaling, which is mediated by nuclear factor kappa B (NF- κ B) and PI3K–AKT signaling. Furthermore, intra-articular injection of SHP099 significantly attenuated OA progression, including joint synovitis and cartilage damage. These findings indicated that SHP2 might be a therapeutic target for the treatment of OA.

2. Materials and methods

2.1. Clinical specimen

Human OA synovial tissues were obtained from patients who had undergone total knee replacement surgery. Normal synovial tissues were obtained from donors who underwent lower limb amputation due to traffic accidents and had no history of arthritic diseases. This study was approved by the Ethical Committee of the Nanjing Drum Tower Hospital, the Affiliated Hospital of Nanjing University Medical School (2020-156-01). The privacy rights of human subjects were always be observed and the informed consent was obtained for experimentation with human subjects.

2.2. Animals

All animal experiments were authorized by the Animal Care and Use Committee of Nanjing Drum Tower Hospital, the affiliated hospital of Nanjing University (2019AE01120). We have complied with all rules and regulations. *Shp2^{fl/fl}* mice were crossed with *Lyz^{Cre}* mice on the C57BL/6 background for more than two generations to generate *Lyz^{Cre}; Shp2^{fl/fl}* mice as previously described¹⁸. *Shp2* was conditionally knocked out in macrophages of *Lyz^{Cre}; Shp2^{fl/fl}* mice, genotype identification was performed, and SHP2 protein was knocked out in BMDMs of *Lyz^{Cre}; Shp2^{fl/fl}* mice (Supporting Information Fig. S1A and S1B). OA was induced in 8-week-old male cKO and wild-type (WT) mice by DMM surgery as previously described¹⁹. After exposure to a 3-mm longitudinal incision over the distal patella to the proximal tibial plateau, the medial meniscotibial ligament (MMTL) was sheared to make the medial meniscus unstable. At 6 weeks after surgery, mice were euthanized for collection of joint tissues. Twenty-four C57BL/6 mice were purchased from the Animal Center of Nanjing Medical University (Nanjing, China). After one week of adaptive feeding, the mice were randomly divided into sham, SHP099, DMM or DMM + SHP099 groups. DMM surgery was performed in the DMM and DMM + SHP099 groups, and two weeks later, intra-articular injection of 10 μ L of 20 μ mol/L SHP099 (MCE) was performed twice a week in the

SHP099 and DMM+SHP099 groups, while the remaining groups were injected with 10 μ L phosphate-buffered saline (PBS).

2.3. Cell culture condition and transfection

RAW264.7 cells were purchased from the Cell Bank of Type Culture Collection of the Chinese Academy of Science (Shanghai, China). BMDMs were obtained and cultured as described previously^{20,21}. Cells were cultured in Dulbecco's modified Eagle's medium (DMEM, Gibco) with 10% Fetal Bovine Serum (FBS, Gibco) and 1% penicillin and streptomycin (Gibco) at 37 °C with 5% CO₂. Lentivirus was purchased from GeneChem (Shanghai, China), and cells were transfected according to the manufacturer's requirements.

To evaluate the role of SHP2 in M1 macrophage polarization, 100 ng/mL LPS (Sigma—Aldrich) was used to induce M1 macrophage polarization, and 20 μ mol/L SHP099 was used to inactivate the SHP2 protein. The M1 macrophage surface marker CD80 (Biolegend) was analysed using a Flow Cytometer (BD Accuri C6 Plus).

2.4. Western blotting

Total protein was extracted using RIPA Lysis Buffer (Solarbio) with 1 mmol/L phenylmethanesulfonyl fluoride (Solarbio) and 1 mmol/L phosphatase inhibitor cocktail (Bimake). Nuclear and cytoplasmic proteins were extracted using a Nucleoplasmic Protein Extraction Kit (Solarbio), and protein concentrations were measured by the BCA Assay Kit (Thermo Scientific). A 10% (*w/v*) SDS-polyacrylamide gel was used to separate proteins (EpiZyme), which were transferred onto polyvinylidene fluoride membranes (Bio-Rad). After blocking with 5% (*w/v*) milk (Bio-Rad) for 1 h at 37 °C, the membrane was incubated with primary antibodies overnight at 4 °C. A horseradish peroxidase-conjugated goat anti-rabbit/mouse IgG (Biosharp) was used as a secondary antibody. All images were obtained using a Western Blotting Imaging System (Tanon).

2.5. Quantitative real-time polymerase chain reaction (qPCR)

TRIzol reagent (Thermo Fisher Scientific) was used to extract RNA from cells. qPCR was conducted in a 20 μ L system using the SYBR Green q-PCR Kit (Vazyme) on a Light Cycler (Roche) with the primers presented in [Supporting Information Table S1](#).

2.6. Histological analysis

Human synovium was fixed with 4% paraformaldehyde (PFA) for 48 h. The total knee joints of mice were decalcified with 10% EDTA at a 7.4 pH for 21 days. They were then embedded in paraffin and cut into 3-micrometer-thick sections for haematoxylin and eosin (H&E) staining and Safranin O/Fast green staining. The synovitis score was evaluated for synovial lining cell thickness (0–3) and synovial stroma density (0–3)²². The Osteoarthritis Research Society International (OARSI) score²³ was evaluated for cartilage degradation. Each section of the histology specimen was evaluated by double-blinded, independent observers.

2.7. Immunohistochemistry and immunofluorescence

After being dewaxed and rehydrated with gradient alcohol, the sections were rinsed with 3% hydrogen peroxide to inactivate

endogenous peroxidases. After antigen retrieval using 0.1% Pepsin (Sigma), the sections were blocked with goat serum (Gibco) for 1 h at 37 °C and incubated with primary antibodies overnight at 4 °C. Immunohistochemistry sections were incubated with horseradish peroxidase-conjugated secondary antibody (Biosharp) for 1 h at 37 °C. The positive cells were visualized using 3,3-diaminobenzidine (Typng). Images were received by Optical Microscope (Zeiss). Immunofluorescence sections were incubated with FITC- or TRITC-conjugated secondary antibodies for 1 h at 37 °C, and then the nuclei were stained with 4,6-diamidino-2-phenylindole (Abcam) for 4 min. Images were obtained on a Fluorescence Microscope (Zeiss, Germany). For cytological immunofluorescence, the cells were fixed in 4% PFA. After blocking with 5% bovine serum albumin (BSA) for 1 h, the primary antibody was incubated overnight, and the following procedures were the same as those for immunofluorescence.

2.8. Antibodies

The following antibodies were used: mouse anti-F4/80 (Santa Cruz), rabbit anti-iNOS (Cell Signaling Technology), mouse anti-CD80 (Invitrogen Antibodies), rabbit anti-CD206 (Abcam), rabbit anti-SHP2 (Cell Signaling Technology), rabbit anti-COL2 (Abcam), rabbit anti-COL10 (Abcam), rabbit anti-MMP3 (Proteintech), rabbit anti-COX2 (Cell Signaling Technology), rabbit anti-GAPDH (Cell Signaling Technology), rabbit anti-p-P65 (Cell Signaling Technology), rabbit anti-P65 (Cell Signaling Technology), rabbit anti- β -actin (Cell Signaling Technology), rabbit anti-histone H3 (Cell Signaling Technology), rabbit anti-p-AKT (Cell Signaling Technology), rabbit anti-AKT (Cell Signaling Technology), and rabbit anti-p-IKK α / β (Cell Signaling Technology).

2.9. Enzyme-linked immunosorbent assay (ELISA)

The tumor necrosis factor (TNF)- α and IL-6 levels in the supernatant of cultured RAW264.7 cells and BMDMs were investigated using ELISA Kits (R&D Systems) according to the manufacturer's instructions. The absorbance at 450 nm was detected by a Microplate Reader (Thermo Scientific).

2.10. RNA sequence (RNA-seq)

Total RNA was extracted from RAW264.7 cells after LPS treatment with or without SHP099 ($n = 3$) for one day. They were submitted to GeneChem company (Shanghai, China) to acquire the FPKM values of all genes. Pearson's correlation analysis was performed, and heatmaps were generated. In our studies, differentially expressed genes (DEGs) were defined as fold changes > 1.4 and $P < 0.05$. Kyoto Encyclopedia of Genes and Genomes (KEGG) analysis was performed to evaluate the biological function of DEGs.

2.11. Statistical analysis

All results were observed by different researchers. Differences between two groups were analysed by paired or unpaired Student's *t* test (parametric or nonparametric test), while the results of three or four groups were analysed by one-way analysis of variance (ANOVA, parametric test). The nonparametric data (such as OARSI scores and synovitis scores) were analysed using the Kruskal–Wallis test with multiple comparisons. All graphics were

made by Prism 8 (GraphPad Software Inc.). The results are presented as the mean \pm standard error of mean (SEM), and $P < 0.05$ were considered as statistically significant ($*P < 0.05$, $**P < 0.01$), ns represents no significance.

3. Results

3.1. M1 macrophages are significantly increased in the synovium from OA patients and DMM mice

To explore the role of synovial macrophages in OA, we examined the synovitis score and macrophage polarization in the synovium of OA patients. Consistent with a previous study⁷, the OA synovium presented a higher synovitis score, which was accompanied by increased cell infiltration and synovial thickness (Supporting Information Fig. S2A and S2B). In OA synovium, F4/80

(macrophage marker)-positive cells were significantly increased, which was accompanied by an elevated proportion of inducible nitric oxide synthase (iNOS) (M1 macrophage marker)- and CD80 (M1 macrophage marker)-positive cells (Fig. S2C and S2D). However, the proportion of CD206 (M2 macrophage marker)-positive cells was lower than that of iNOS-positive cells, with no significant difference observed between the normal and OA groups (Supporting Information Fig. S3). We also investigated synovitis and macrophage polarization in a DMM-induced OA mouse model. The cell infiltration and tissue proliferation of the synovium of DMM mice were observed, and their synovitis scores were significantly elevated from 2 weeks to 8 weeks after DMM surgery (Fig. S2E and S2F). Similar to OA patients' synovium, the accumulation of macrophages and the percentage of M1 macrophages were significantly increased in 6-week DMM mice (Fig. S2G and S2H).

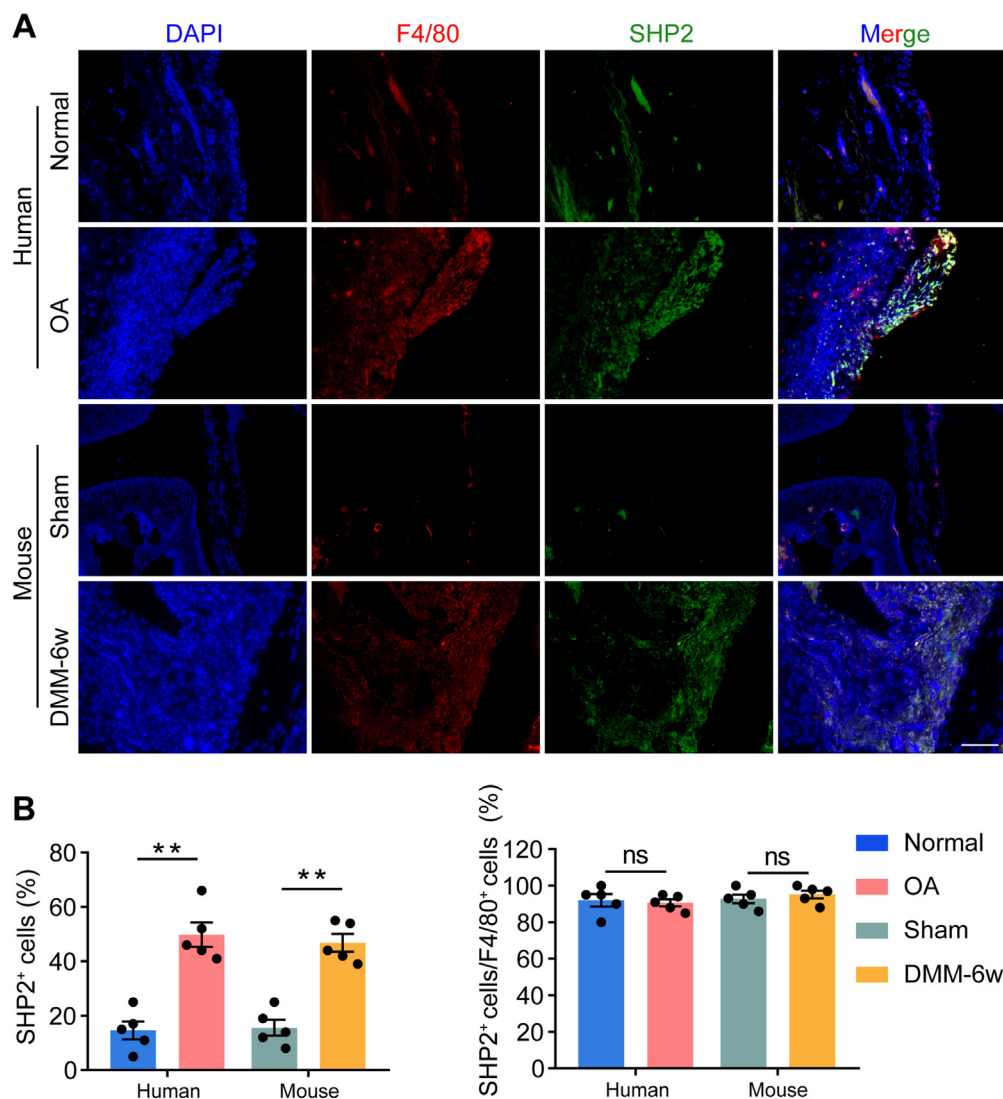


Figure 1 SHP2 expression and located cells in the synovium of OA patients and DMM mice. (A) Representative images of immunofluorescence of src-homology 2-containing protein tyrosine phosphatase 2 (SHP2), F4/80 and their colocalization in normal synovium and osteoarthritis (OA) synovium from human, and the representative immunofluorescence images of SHP2, F4/80 and their colocalization in the synovium of sham and 6-week destabilization of medial meniscus (DMM) mice. Scale bar: 100 μ m. (B) Quantification of the proportion of SHP2-positive cells in synovial cells and F4/80-positive cells. Two-way analysis of variance (ANOVA) with Tukey's multiple comparison test. All data are shown as the mean \pm SEM, $n = 5$; $**P < 0.01$, ns represents no significance.

3.2. SHP2 is located in the accumulated macrophages and upregulated in the synovium from OA patients and DMM mice

To determine whether SHP2 participated in the synovitis of OA, SHP2 expression and its colocalization with a macrophage marker (F4/80) were examined. Compared to that in normal subjects, SHP2 expression in the synovium was significantly elevated in OA patients. In addition, SHP2 was mostly located in the accumulated

macrophages. Similar results were observed in the synovium of DMM mice (Fig. 1A and B).

3.3. SHP2 deletion in macrophages attenuates OA by inhibiting M1 macrophage polarization

Compared to *Shp2^{fl/fl}* mice, the cartilage degeneration of *Shp2^{fl/fl}; Lyz^{Cre}* mice was significantly attenuated during the OA process.

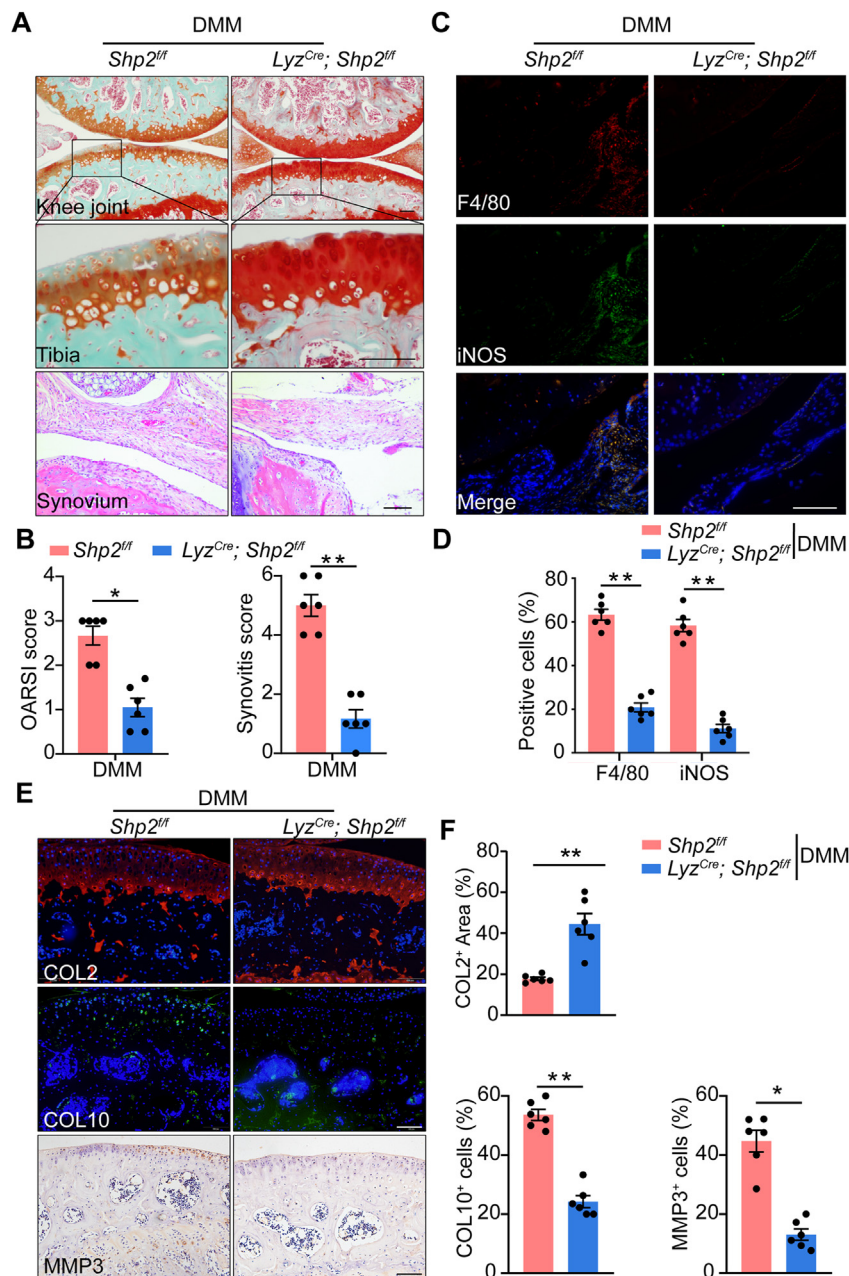


Figure 2 Conditional *Shp2* deletion in macrophages attenuated the severity of osteoarthritis. (A) Representative images of Safranin O/Fast Green of the cartilage and synovium from *Shp2^{fl/fl}* and *Shp2^{fl/fl}; Lyz^{Cre}* mice. Scale bar: 100 μ m. (B) Quantification of the Osteoarthritis Research Society International (OARSI) score and Synovitis score of *Shp2^{fl/fl}* ($n = 6$) and *Shp2^{fl/fl}; Lyz^{Cre}* ($n = 6$) mice. Unpaired Student's *t*-test (non-parametric test), $**P < 0.01$. (C) Representative images of immunofluorescence of F4/80 and iNOS in the synovium from *Shp2^{fl/fl}* and *Shp2^{fl/fl}; Lyz^{Cre}* mice. Scale bar: 100 μ m. (D) Quantification of the proportion of F4/80- and iNOS- positive cells in the synovium from *Shp2^{fl/fl}* ($n = 6$) and *Shp2^{fl/fl}; Lyz^{Cre}* ($n = 6$) mice. Unpaired Student's *t*-test (parametric test), $**P < 0.01$. (E) Representative images of immunofluorescence of collagen II (COL2), collagen X (COL10), and matrix metalloproteinase 3 (MMP3). Scale bar: 100 μ m. (F) Quantification of the proportion of the positive area of COL2, the proportion of cells expressing COL10 and MMP3 in the cartilage of *Shp2^{fl/fl}* and *Shp2^{fl/fl}; Lyz^{Cre}* mice ($n = 6$). Unpaired Student's *t*-test (parametric test); $*P < 0.05$, $**P < 0.01$. All Data are shown as the mean \pm SEM.

The cell infiltration of synovium from the cKO mice was decreased (Fig. 2A). The synovitis and OARSI scores of *Shp2^{fl/fl}; Lyz^{Cre}* mice were lower (Fig. 2B). Moreover, decreased macrophage accumulation was shown in the cKO mice, which was accompanied by a lower rate of M1 macrophage markers, including iNOS and CD80 (Fig. 2C and D, Supporting Information Fig. S4A and S4B). Compared to *Shp2^{fl/fl}* mice, collagen II (COL2) was elevated in the cartilage of *Shp2^{fl/fl}; Lyz^{Cre}* mice at 6 weeks after DMM surgery, while the hypertrophic cartilage marker collagen X (COL10) was decreased. Furthermore, the expression of the cartilage degradation enzyme matrix metalloproteinases 3 (MMP3) was significantly reduced when *Shp2* was conditional deleted, which may explain the cartilage protection effect in *Shp2^{fl/fl}; Lyz^{Cre}* mice (Fig. 2E and F).

3.4. SHP099 treatment inhibits LPS-induced M1 macrophage polarization

To determine the purity of RAW264.7 cells and BMDMs, F4/80 (macrophage surface marker) of RAW264.7 cells and BMDMs was identified using flow cytometry (Supporting Information Fig. S5A). After stimulation with LPS for 3 h, the *Shp2* mRNA level was significantly elevated in RAW264.7 cells (Fig. S5B). BMDMs from *Lyz^{Cre}; Shp2^{fl/fl}* mice attenuated LPS-induced IL-6 and TNF- α release (Supporting Information Fig. S6A and S6B) and M1-related mRNA expression (Fig. S6C). To determine the impact of allosteric SHP2 inhibitor on macrophage polarization *in vitro*, we applied SHP099, an SHP2 allosteric inhibitor, to RAW264.7 cells and BMDMs stimulated with LPS for 24 h. The assessment of the expression level of M1 macrophage markers by flow cytometry revealed that the proportion of CD80⁺ cells decreased remarkably after SHP099 treatment (Fig. 3A). Similarly, inhibition of SHP2 in RAW264.7 cells and BMDMs significantly downregulated M1 macrophage-expressed inflammatory genes [*Il1b*, *Il6*, *Tnfa*, *CXC chemokine ligand-10 (Cxcl10)* and *iNos*] (Fig. 3B and C). ELISA results showed that SHP099 significantly decreased the secretion of LPS-induced inflammatory cytokines (TNF- α and IL-6) (Fig. 3D and E). Furthermore, M1 macrophage-related proinflammatory proteins [iNOS and cyclooxygenase 2 (COX2)] were decreased after SHP099 treatment (Fig. 3F and G). Furthermore, SHP2 overexpression enhanced the expression of iNOS and COX2 (Fig. 3H). To avoid the off-target effect of SHP099, we also found that another SHP2 allosteric inhibitor, SHP836, inhibited M1 macrophage-related inflammatory protein and gene expression (Supporting Information Fig. S7A and S7B).

3.5. SHP099 downregulates the TLR pathway by inhibiting MyD88-dependent transduction

To identify the underlying mechanism by which SHP099 modulates M1 macrophage polarization, we performed RNA sequencing (RNA-seq) analysis on RAW264.7 cells stimulated by LPS with or without SHP099 treatment (Fig. 4A). A total of 8528 DEGs were identified between the vehicle (V) and LPS (L) groups, and 1380 DEGs were identified between the LPS (L) group and LPS+SHP099 (LS) group (Fig. 4B). Pathway enrichment analysis identified significant enrichment of DEGs, such as TLR signaling, NF- κ B signaling and PI3K-AKT signaling (Fig. 4C). LPS is a classic stimulator of TLR signaling, and the myeloid differentiation primary response protein 88 (MyD88)-dependent pathway is a key pathway involved in TLR signaling and IL-1 receptor family signaling, which includes the NF- κ B²⁴

and PI3K-AKT pathways²⁵. SHP099 treatment significantly downregulated TLR and NF- κ B signaling, with several related genes stimulated by LPS, such as *Cxcl2*, *Nfkb2*, *Bcl2a1a*, and *Il1b* (Fig. 4D and E). Moreover, the expression of many PI3K-AKT-related genes was also decreased in the SHP099 group (Fig. 4F). LPS stimulation significantly elevated the protein levels of p-IKK α/β , p-P65, and p-AKT, which decreased after SHP099 treatment in RAW264.7 cells and BMDMs (Fig. 4G and H). Moreover, the translocation of P65 into the nucleus was observed after 3 or 6 h of LPS stimulation and was inhibited by SHP099 in RAW264.7 cells (Supporting Information Fig. S8A). Immunofluorescence revealed that SHP099 partially inhibited the translocation of P65 induced by LPS in RAW264.7 cells (Fig. S8B and S8C). These results indicate that SHP099 attenuates the TLR pathway and its downstream signaling pathways, including the NF- κ B and PI3K-AKT pathways.

3.6. Inhibition of the PI3K and NF- κ B pathways inhibits M1 macrophage polarization

To investigate whether the PI3K and NF- κ B pathways mediate SHP099-induced macrophage polarization, PI3K (LY294002) and NF- κ B (JSH23) inhibitors were used *in vitro*. The rate of CD80⁺ cells was significantly decreased after LY294002 and JSH23 treatment in RAW264.7 cells and BMDMs (Fig. 5A). The mRNA expression of M1 macrophage markers (*iNos*, *Il1b*, *Il6*, *Tnfa* and *Cxcl10*) was also decreased after LY294002 and JSH23 treatment in RAW264.7 cells and BMDMs (Fig. 5B and C), and the inhibition of the M1 phenotype induced by SHP099 was not promoted in RAW264.7 cells in which the PI3K-AKT and NF- κ B pathways were blocked (Supporting Information Fig. S9).

3.7. Intra-articular injection of SHP099 alleviates OA by inhibiting M1 macrophage polarization

To examine whether SHP099 could inhibit M1 macrophage polarization and alleviate OA *in vivo*, intra-articular injection of SHP099 was performed in a mouse DMM model. After intra-articular injection of SHP099, the abundance of cartilage extracellular matrix increased compared to that in the DMM group. Cell infiltration of the synovium was remarkably decreased after SHP099 administration (Fig. 6A). The OARSI score and synovitis score decreased significantly (Fig. 6B). Consistent with the synovitis score, there was a substantial reduction in the proportion of F4/80-, iNOS-, and CD80-positive cells in the synovium following SHP099 injection (Fig. 6C and D, Supporting Information Fig. S10A and S10B). Furthermore, the expression of COL2 was elevated in the cartilage of the SHP099 group after DMM surgery, while COL10 was decreased. Furthermore, the expression of MMP3 was significantly reduced (Fig. 6E and F), indicating that the SHP2 allosteric inhibitor could be a potential therapeutic drug for OA.

4. Discussion

In this study, we demonstrated for the first time that increased SHP2 was mostly located in accumulated macrophages in the synovium of OA patients and OA model mice, thus indicating its potential role in OA. Conditional deletion of *Shp2* in macrophages could decrease M1 macrophage polarization, attenuate synovitis and decrease cartilage degradation during OA progression. Moreover, SHP2 inhibition reduced LPS-induced M1 macrophage polarization *via* the TLR signaling pathway *in vitro*.

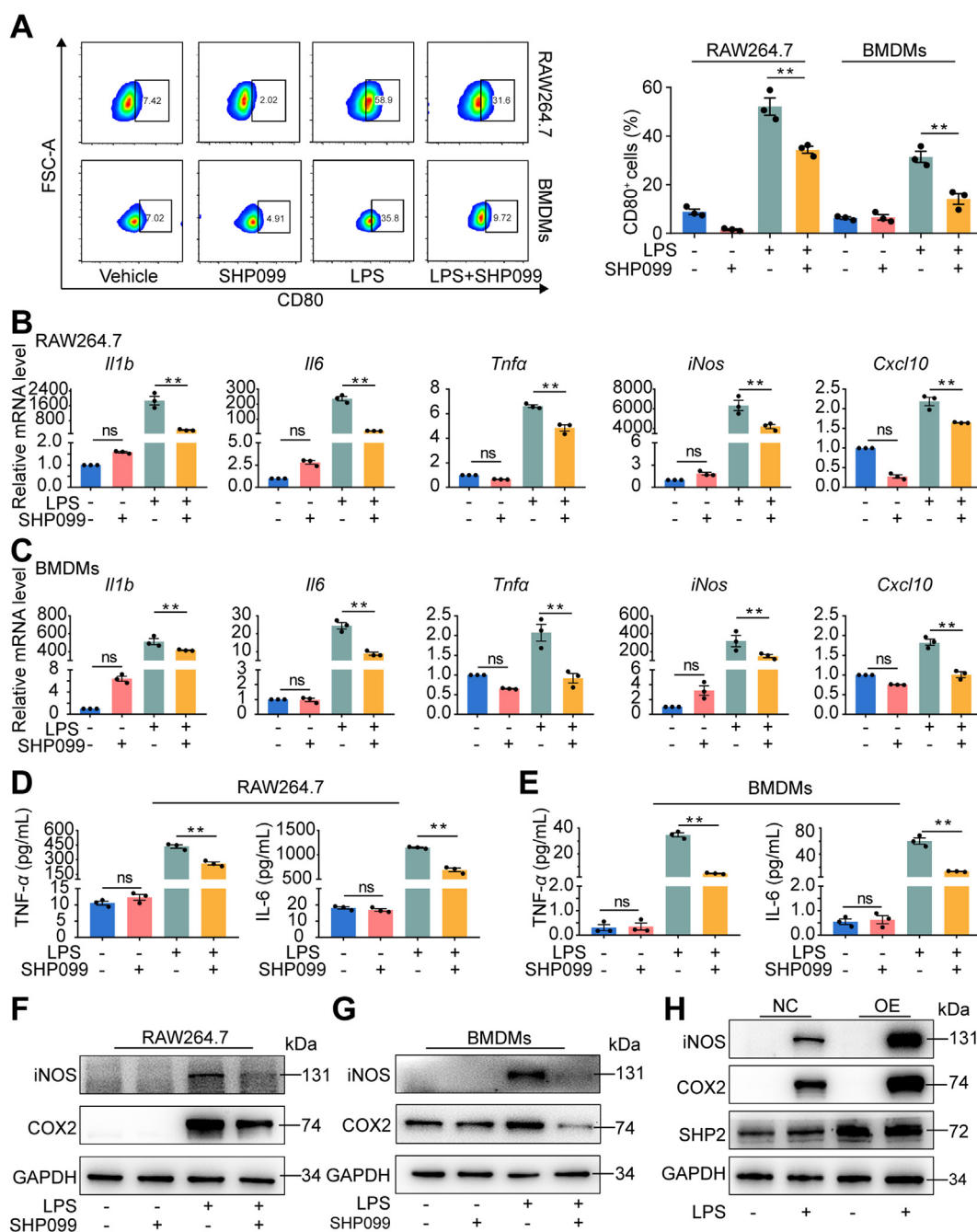


Figure 3 SHP099 inhibited macrophage M1 polarization and inflammatory cytokines secretion during LPS-induced inflammation for 24 h. (A) Flow cytometry for detection and quantitative analysis of CD80⁺ cells after the treatment of lipopolysaccharide (LPS) with or without SHP099 for 24 h in RAW264.7 cells and bone marrow-derived macrophages (BMDMs) ($n = 3$). One-way ANOVA with Tukey's multiple comparison test; $**P < 0.01$. (B) qPCR analysis of mRNA of M1-related genes, interleukin-1 β (*Il1b*), *Il6*, tumor necrosis factor α (*Tnfa*), inducible nitric oxide synthase (*iNos*) and CXC chemokine ligand-10 (*Cxcl10*) in RAW264.7 cells after LPS stimulation with or without SHP099 treatment for 24 h ($n = 3$). One-way ANOVA with Tukey's multiple comparison test; $**P < 0.01$, ns represents no significance. (C) qPCR analysis of mRNA of M1-related genes, *Il1b*, *Il6*, *Tnfa*, *iNos* and *Cxcl10* in BMDMs after LPS stimulation with or without SHP099 treatment for 24 h ($n = 3$). One-way ANOVA with Tukey's multiple comparison test; $**P < 0.01$, ns represents no significance. (D) Enzyme-linked immunosorbent assay (ELISA) results of TNF- α and IL-6 secretion of RAW264.7 cells after LPS stimulation with or without SHP099 treatment for 24 h ($n = 3$). One-way ANOVA with Tukey's multiple comparison test; $**P < 0.01$, ns represents no significance. (E) ELISA results of TNF- α and IL-6 secretion of BMDMs cells after LPS stimulation with or without SHP099 treatment for 24 h. One-way ANOVA with Tukey's multiple comparison test. $**P < 0.01$. (F) Western blot analysis of iNOS and cyclooxygenase 2 (COX2) in RAW264.7 after LPS stimulation with or without SHP099 treatment for 48 h. (G) Western blot analysis of iNOS and COX2 in BMDMs after LPS stimulation with or without SHP099 treatment for 48 h. (H) Western blot analysis of iNOS and COX2 in RAW264.7 after LPS stimulation with over-expression (OE) of SHP2 or not (NC) for 48 h. All data are shown as the mean \pm SEM.

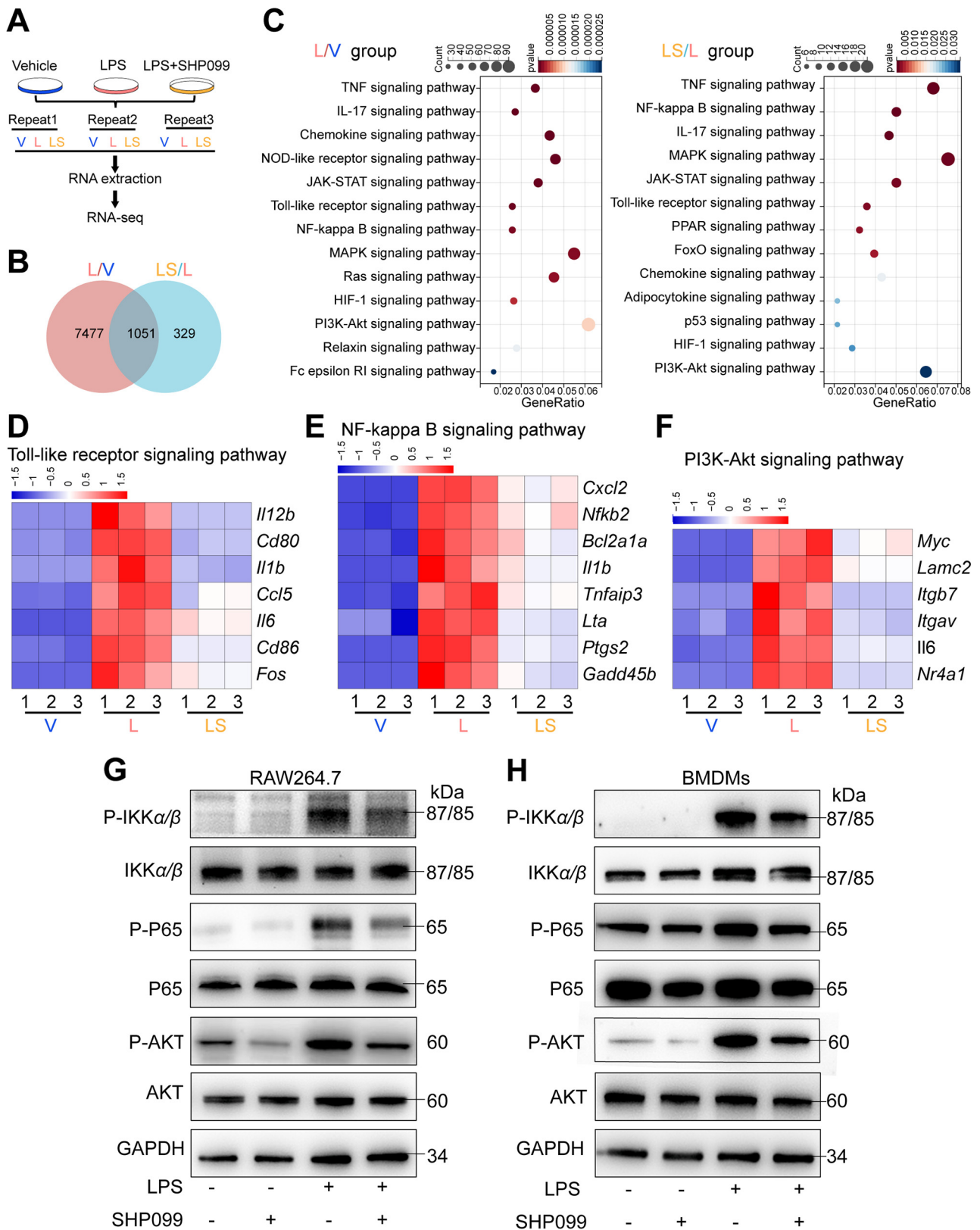


Figure 4 SHP099 inhibited Toll-like signaling (TLR) pathway, including its downstream pathways, including nuclear factor kappaB (NF- κ B) pathway, and PI3K-AKT pathway. (A) Schematic diagram for RNA-sequence analysis. (B) Venn diagram. (C) Encyclopedia of Genes and Genomes (KEGG) analysis of the biological function of differentially expressed genes (DEGs). (D) DEGs in the TLR signaling pathway. (E) DEGs in the NF- κ B signaling pathway. (F) DEGs in the PI3K-AKT signaling pathway. (G) Western blot analysis of p-IKK α/β , IKK α/β , p-P65, P65, p-AKT, AKT, GAPDH after LPS stimulation with or without SHP099 treatment in RAW264.7 cells. (H) Western blot analysis of p-IKK α/β , IKK α/β , p-P65, P65, p-AKT, AKT, GAPDH after LPS stimulation with or without SHP099 treatment in BMDMs.

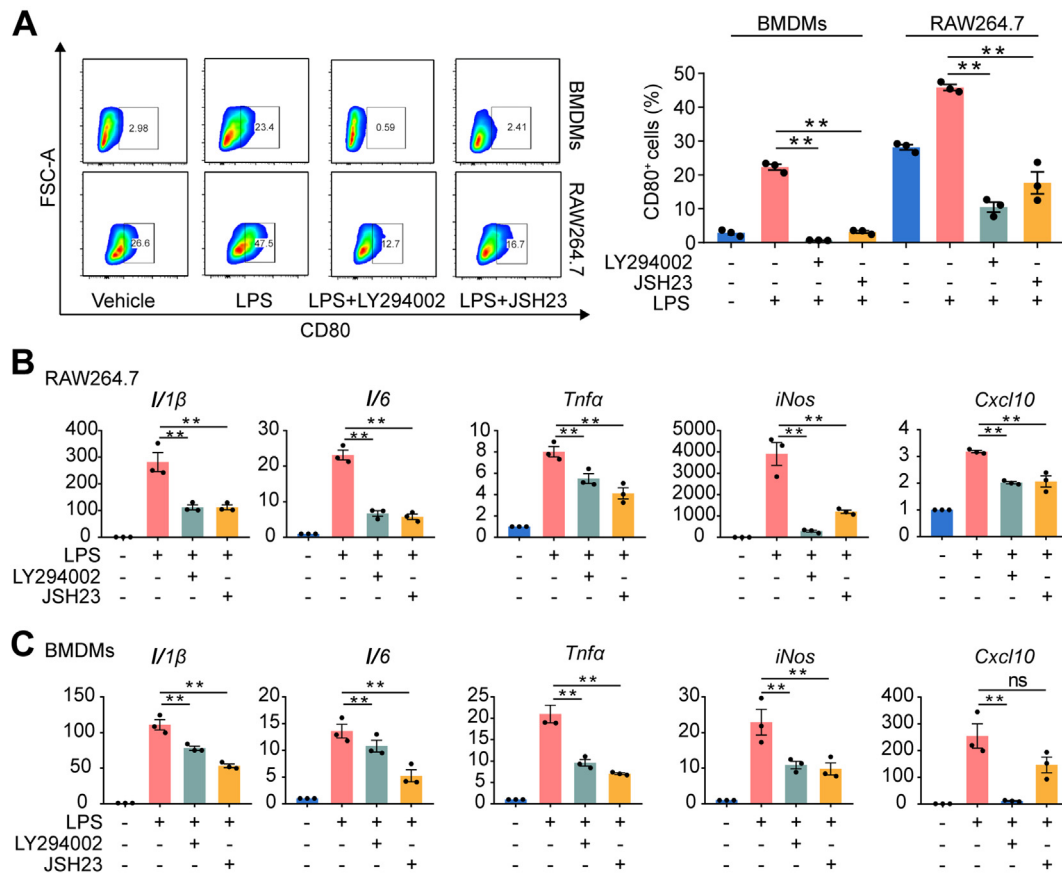


Figure 5 Inhibition of NF- κ B pathway and PI3K pathway inhibited macrophage M1 polarization. (A) Flow cytometry for detection and quantitative analysis of CD80-positive cells after the treatment of LPS with or without treatment of LY294002 and JSH23 for 24 h in RAW264.7 cells and BMDMs ($n = 3$). One-way ANOVA with Tukey's multiple comparison test, $**P < 0.01$. (B) qPCR analysis of mRNA of M1-related genes, *I/1b*, *I/6*, *Tnfa*, *iNos* and *Cxcl10* in RAW264.6 cells after LPS stimulation with or without LY294002 and JSH23 treatment for 24 h ($n = 3$). One-way ANOVA with Tukey's multiple comparison test, $**P < 0.01$. (C) qPCR analysis of mRNA of M1-related genes, *I/1b*, *I/6*, *Tnfa*, *iNos* and *Cxcl10* in BMDMs after LPS stimulation with or without LY294002 and JSH23 treatment for 24 h ($n = 3$). One-way ANOVA with Tukey's multiple comparison test, $**P < 0.01$. All data are shown as the mean \pm SEM.

Intra-articular injection of SHP099 alleviated OA progression in a mouse DMM model. These results provide a new perspective for intervention in the OA process by modulating macrophage polarization (Fig. 7).

Studies have shown that enhanced synovial M1 macrophage polarization is responsible for the increased severity of OA⁷. Consistent with previous studies^{7,22}, we found increased synovitis score and highly infiltrated M1 macrophages in the synovium of OA patients. Compared to the collagenase-induced OA model, the DMM-induced OA mouse model was described as a low synovial-activation OA model²⁶, but we found that in the DMM model, the synovitis scores were also increased significantly from 2 weeks after DMM surgery, thus indicating that synovitis participated in the process of OA progression from the early to late phases. Furthermore, macrophage accumulation and M1 polarization in the synovium of the DMM-induced OA mouse model were also observed. The DMM model simulates the pathological process of OA well, and these results suggested that synovitis and macrophage polarization played a vital role in the development of OA.

A recent study revealed that SHP2 could promote the invasion and survival of synovial fibroblasts during RA²⁷, but

whether SHP2 participates in macrophage function and polarization during the pathologic process of OA was not investigated. Compared to the WT mice, the cartilage degradation of the cKO mice was significantly decreased, which might be associated with the lower expression of degrading enzymes, such as MMP3. Furthermore, as we expected, macrophage accumulation in cKO mice was significantly attenuated. At the same time, the proportion of M1 macrophages was decreased, which might explain why cartilage degradation decreased. Intra-articular injection of SHP099 also has an ideal therapeutic effect. Several studies have tried to influence the OA process by interfering with the function of macrophages, such as physical therapy represented by low-intensity pulsed ultrasound²⁸ and small molecule drugs represented by kinsenoside²⁹ and rapamycin⁷. Therefore, finding a specific target modulating macrophage polarization will provide new ideas regarding potential treatments for OA, and our results showed that SHP2 is a new ideal target through which to influence the polarization of macrophages during the OA process.

To explore the underlying mechanism of SHP2 on macrophage polarization, RAW 264.7 cells, a mouse macrophage cell line that is widely used as M0 macrophages³⁰ and BMDMs, were used. Under

LPS stimulation, SHP099 treatment inhibited M1 macrophage polarization. LPS is a classic stimulator of TLRs, whose downstream signaling is regulated by MyD88-and TRIF-dependent pathways³¹. Recent studies revealed that the MyD88 pathway modulated the M1 polarization of macrophages^{32,33}, but whether this process is involved in SHP2-regulated macrophage polarization is unknown. According to our RNA-seq results, SHP099 significantly attenuated LPS-induced TLR signaling, and p-P65³⁴ and p-AKT³⁵ were decreased after SHP099 treatment, which are key proteins in the

TLR/MyD88 proinflammatory pathway. These results showed that SHP2 might be a possible modulator of the TLR/MyD88 pathway.

There are several limitations of this study. First, we did not evaluate the effect of *Shp2* conditional deletion on other OA models, such as spontaneous OA, which would hamper a more comprehensive understanding of the role of SHP2 in OA. Second, we did not evaluate the periarticular osteophyte formation of mice and hence might ignore the possible role of SHP2 in bone remodelling.

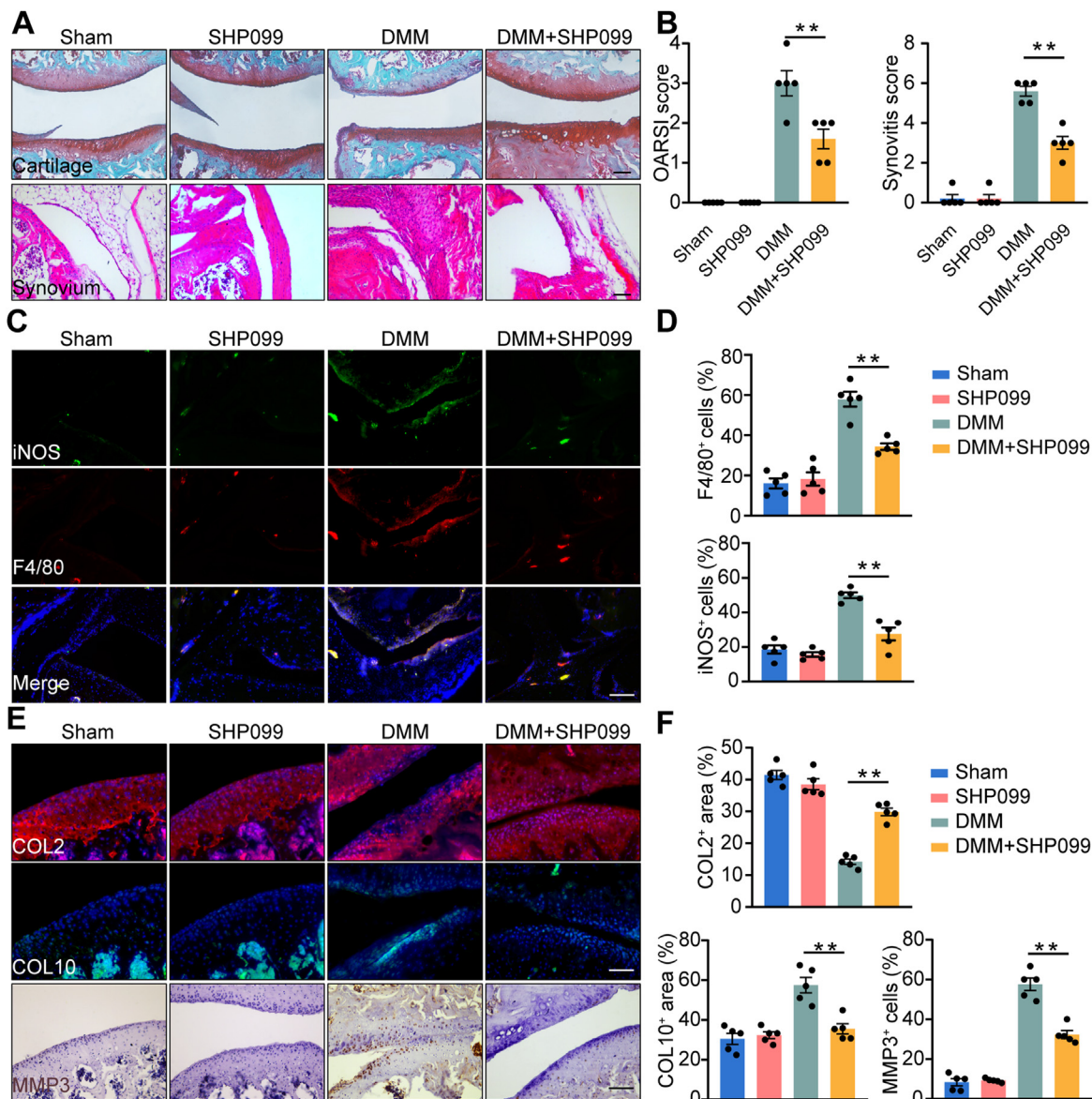


Figure 6 Intra-articular injection of SHP099 attenuated DMM-induced OA progression in mice model. (A) Representative images of Safranin O/Fast Green of the cartilage and H&E staining of synovium from mice divided into four groups, including Sham group, intra-articular injection of SHP099 group, DMM group and DMM with injection of SHP099 group. Scale bar: 100 μ m. (B) Quantification of synovitis score and OARSI score of four groups ($n = 5$). One-way ANOVA with Tukey's multiple comparison test, $^{***}P < 0.01$. (C) Representative images of immunofluorescence of F4/80 and iNOS in the synovium from mice in four groups. Scale bar: 100 μ m. (D) Quantification of the proportion of F4/80- and iNOS- positive cells in the synovium from mice in four groups ($n = 5$). One-way ANOVA with Tukey's multiple comparison test, $^{***}P < 0.01$. (E) Representative images of immunofluorescence of COL2, COL10 and MMP3. Scale bar: 100 μ m. (F) Quantification of the proportion of the positive area of COL2, the proportion of cells expressing COL10 and the proportion of cells expressing MMP3 in the cartilage of mice divided into four groups ($n = 5$). One-way ANOVA with Tukey's multiple comparison test, $^{***}P < 0.01$. All data are shown as the mean \pm SEM.

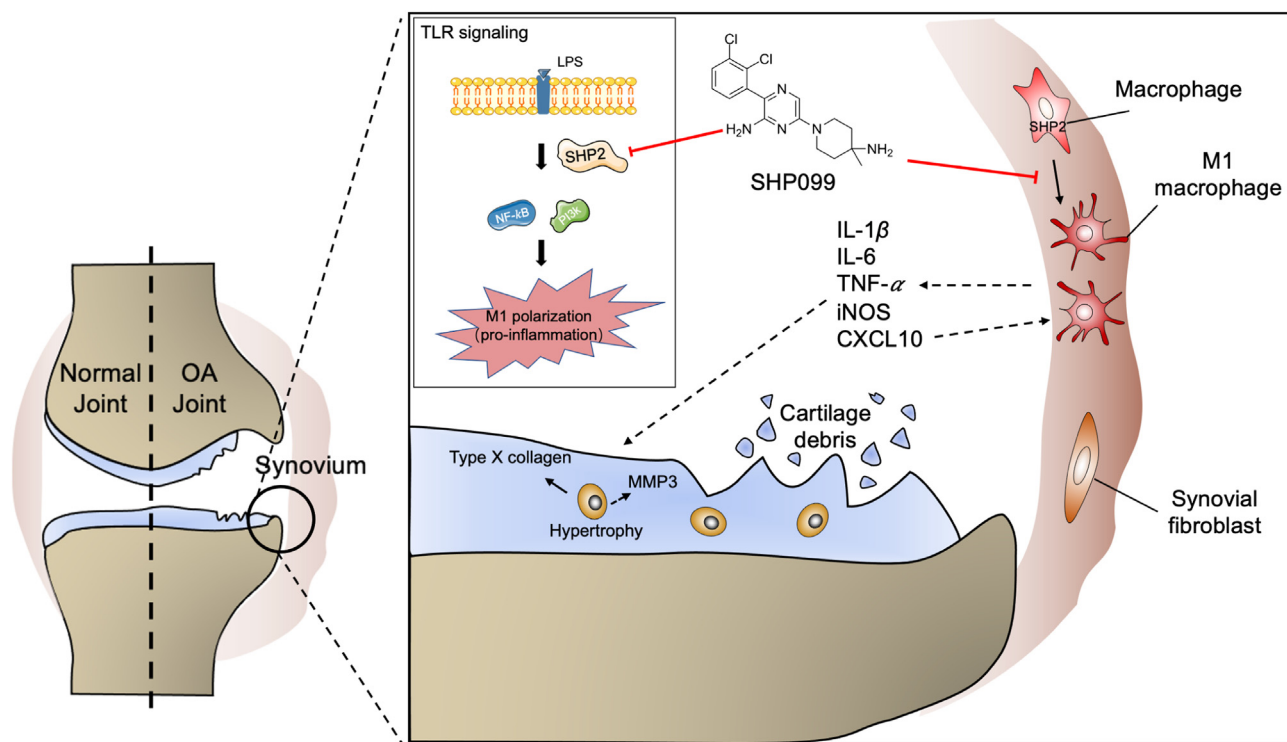


Figure 7 The graphic illustration of the mechanism of SHP2-mediated macrophage polarization in osteoarthritis. SHP2 aggravates M1 macrophage-induced synovitis in OA by inhibiting NF- κ B and PI3K–AKT signal pathway, indicating that targeting macrophagic SHP2 is a promising strategy for OA.

5. Conclusions

To conclude, we found that SHP2 inhibition is a potential therapeutic strategy that can be used to attenuate the severity of OA by repolarizing M1 macrophages in synovial tissues. Future studies are warranted to explore the underlying mechanisms of how SHP2 allosteric inhibitors modulate the transduction of the TLR/MyD88 proinflammatory pathway.

Acknowledgments

We also thank Professor Tao Shi from the Comprehensive Cancer Centre of Nanjing Drum Tower Hospital, the Affiliated Hospital of Nanjing University Medical School & Clinical Cancer Institute of Nanjing University (Nanjing, China) for the help for us. This work was supported by the National Science Foundation of China (NSFC 81802196, 81572129, 81872877, 91853109, and 81772335), Key Program of NSFC (81730067, China), Special Program of Chinese Academy of Science (XDA16020805, China), Jiangsu Provincial Key Medical Center Foundation (China), Jiangsu Provincial Medical Outstanding Talent Foundation (China), and Jiangsu Provincial Key Medical Talent Foundation (China).

Author contributions

Dongquan Shi and Yang Sun conceived and supervised the study. Ziyang Sun, Qianqian Liu performed the cell line experiments and animal experiments and analyzed the data. Zhongyang Lv, Jiawei Li, and Xingquan Xu performed bioinformatics analysis. Heng Sun, Maochun Wang, Kuoyang Sun and Tianshu Shi collected

clinical samples. Zizheng Liu, Guihua Tan, Wenqiang Yan, Rui Wu, Yannick Xiaofan Yang, Shiro Ikegawa, Dongdong Sun, Haibo Cheng and Yuxian Shen gave methodological support and conceptual advice. Ziyang Sun and Qianqian Liu wrote the manuscript. All authors discussed the results and commented on the manuscript.

Conflicts of interest

The authors declare no conflicts of interest.

Appendix A. Supporting information

Supporting data to this article can be found online at <https://doi.org/10.1016/j.apsb.2022.02.010>.

References

1. Woolf AD, Pfleger B. Burden of major musculoskeletal conditions. *Bull World Health Organ* 2003;**81**:646–56.
2. Wei Y, Bai L. Recent advances in the understanding of molecular mechanisms of cartilage degeneration, synovitis and subchondral bone changes in osteoarthritis. *Connect Tissue Res* 2016;**57**:245–61.
3. Baker K, Grainger A, Niu J, Clancy M, Guermazi A, Crema M, et al. Relation of synovitis to knee pain using contrast-enhanced MRIs. *Ann Rheum Dis* 2010;**69**:1779–83.
4. Scanzello CR, Goldring SR. The role of synovitis in osteoarthritis pathogenesis. *Bone* 2012;**51**:249–57.
5. Haraden CA, Huebner JL, Hsueh MF, Li YJ, Kraus VB. Synovial fluid biomarkers associated with osteoarthritis severity reflect macrophage and neutrophil related inflammation. *Arthritis Res Ther* 2019;**21**:146.

6. Mantovani A, Sica A, Sozzani S, Allavena P, Vecchi A, Locati M. The chemokine system in diverse forms of macrophage activation and polarization. *Trends Immunol* 2004;**25**:677–86.
7. Zhang H, Lin C, Zeng C, Wang Z, Wang H, Lu J, et al. Synovial macrophage M1 polarisation exacerbates experimental osteoarthritis partially through R-spondin-2. *Ann Rheum Dis* 2018;**77**:1524–34.
8. Wu CL, McNeill J, Goon K, Little D, Kimmerling K, Huebner J, Kraus V, et al. Conditional macrophage depletion increases inflammation and does not inhibit the development of osteoarthritis in obese macrophage fas-induced apoptosis-transgenic mice. *Arthritis Rheumatol* 2017;**69**:1772–83.
9. Feng GS, Hui CC, Pawson T. SH2-containing phosphotyrosine phosphatase as a target of protein-tyrosine kinases. *Science* 1993;**259**:1607–11.
10. Tajan M, de Rocca Serra A, Valet P, Edouard T, Yart A. SHP2 sails from physiology to pathology. *Eur J Med Genet* 2015;**58**:509–25.
11. Zhang J, Zhang F, Niu R. Functions of SHP2 in cancer. *J Cell Mol Med* 2015;**19**:2075–83.
12. Guo W, Liu W, Chen Z, Gu Y, Peng S, Shen L, et al. Tyrosine phosphatase SHP2 negatively regulates NLRP3 inflammasome activation via ANT1-dependent mitochondrial homeostasis. *Nat Commun* 2017;**8**:2168.
13. Xiao P, Zhang H, Zhang Y, Zheng M, Liu R, Zhao Y, et al. Phosphatase Shp2 exacerbates intestinal inflammation by disrupting macrophage responsiveness to interleukin-10. *J Exp Med* 2019;**216**:337–49.
14. Liu Q, Zhai L, Han M, Shi D, Sun Z, Peng S, et al. SH2 domain-containing phosphatase 2 inhibition attenuates osteoarthritis by maintaining homeostasis of cartilage metabolism via the docking protein 1/uridine phosphorylase 1/uridine cascade. *Arthritis Rheumatol* 2022;**74**:462–74.
15. Chen YN, LaMarche MJ, Chan HM, Fekkes P, Garcia-Fortanet J, Acker MG, et al. Allosteric inhibition of SHP2 phosphatase inhibits cancers driven by receptor tyrosine kinases. *Nature* 2016;**535**:148–52.
16. Zhao M, Guo W, Wu Y, Yang C, Zhong L, Deng G, et al. SHP2 inhibition triggers anti-tumor immunity and synergizes with PD-1 blockade. *Acta Pharm Sin B* 2019;**9**:304–15.
17. Glasson SS, Blanchet TJ, Morris EA. The surgical destabilization of the medial meniscus (DMM) model of osteoarthritis in the 129/SvEv mouse. *Osteoarthritis Cartilage* 2007;**15**:1061–9.
18. Tao B, Jin W, Xu J, Liang Z, Yao J, Zhang Y, et al. Myeloid-specific disruption of tyrosine phosphatase Shp2 promotes alternative activation of macrophages and predisposes mice to pulmonary fibrosis. *J Immunol* 2014;**193**:2801–11.
19. Kuyinu EL, Narayanan G, Nair LS, Laurencin CT. Animal models of osteoarthritis: classification, update, and measurement of outcomes. *J Orthop Surg Res* 2016;**11**:19.
20. Zhang Z, Jiang Y, Zhou Z, Huang J, Chen S, Zhou W, et al. Scavenger receptor A1 attenuates aortic dissection via promoting efferocytosis in macrophages. *Biochem Pharmacol* 2019;**168**:392–403.
21. Li H, Ghazanfari R, Zacharaki D, Lim HC, Scheduling S. Isolation and characterization of primary bone marrow mesenchymal stromal cells. *Ann N Y Acad Sci* 2016;**1370**:109–18.
22. Krenn V, Morawietz L, Burmester GR, Kinne RW, Mueller-Ladner U, Muller B, et al. Synovitis score: discrimination between chronic low-grade and high-grade synovitis. *Histopathology* 2006;**49**:358–64.
23. Zhang H, Wang H, Zeng C, Yan B, Ouyang J, Liu X, et al. mTORC1 activation downregulates FGFR3 and PTH/PTHrP receptor in articular chondrocytes to initiate osteoarthritis. *Osteoarthritis Cartilage* 2017;**25**:952–63.
24. Zhou M, Xu W, Wang J, Yan J, Shi Y, Zhang C, et al. Boosting mTOR-dependent autophagy via upstream TLR4–MyD88–MAPK signalling and downstream NF- κ B pathway quenches intestinal inflammation and oxidative stress injury. *EBioMedicine* 2018;**35**:345–60.
25. Yan J, Li J, Zhang L, Sun Y, Jiang J, Huang Y, et al. Nrf2 protects against acute lung injury and inflammation by modulating TLR4 and Akt signaling. *Free Radic Biol Med* 2018;**121**:78–85.
26. Schelbergen RF, Geven EJ, van den Bosch MH, Eriksson H, Leanderson T, Vogl T, et al. Prophylactic treatment with S100A9 inhibitor paquinimod reduces pathology in experimental collagenase-induced osteoarthritis. *Ann Rheum Dis* 2015;**74**:2254–8.
27. Ganesan R, Rasool M. Interleukin 17 regulates SHP-2 and IL-17RA/STAT-3 dependent Cyr61, IL-23 and GM-CSF expression and RANKL mediated osteoclastogenesis by fibroblast-like synoviocytes in rheumatoid arthritis. *Mol Immunol* 2017;**91**:134–44.
28. Uddin SMZ, Komatsu DE. Therapeutic potential low-intensity pulsed ultrasound for osteoarthritis: pre-clinical and clinical perspectives. *Ultrasound Med Biol* 2020;**46**:909–20.
29. Zhou F, Mei J, Han X, Li H, Yang S, Wang M, et al. Kinsenoside attenuates osteoarthritis by repolarizing macrophages through inactivating NF- κ B/MAPK signaling and protecting chondrocytes. *Acta Pharm Sin B* 2019;**9**:973–85.
30. Zhang BC, Li Z, Xu W, Xiang CH, Ma YF. Luteolin alleviates NLRP3 inflammasome activation and directs macrophage polarization in lipopolysaccharide-stimulated RAW264.7 cells. *Am J Transl Res* 2018;**10**:265–73.
31. Kagan JC, Su T, Horng T, Chow A, Akira S, Medzhitov R. TRAM couples endocytosis of Toll-like receptor 4 to the induction of interferon- β . *Nat Immunol* 2008;**9**:361–8.
32. Liu JT, Wu SX, Zhang H, Kuang F. Inhibition of MyD88 signaling skews microglia/macrophage polarization and attenuates neuronal apoptosis in the hippocampus after status epilepticus in mice. *Neurotherapeutics* 2018;**15**:1093–111.
33. Arora H, Wilcox SM, Johnson LA, Munro L, Eyford BA, Pfeifer CG, et al. The ATP-binding cassette gene *ABCF1* functions as an E2 ubiquitin-conjugating enzyme controlling macrophage polarization to dampen lethal septic shock. *Immunity* 2019;**50**:418–31.e6.
34. Chen YP, Ke LF, Lu JP, Wang JC, Zhu WF, Chen FF, et al. Prevalence and clinical significance of oncogenic CD79B and MYD88 mutations in primary testicular diffuse large B-cell lymphoma: a retrospective study in China. *Oncotargets Ther* 2019;**12**:10165–75.
35. Zhong J, Qiu X, Yu Q, Chen H, Yan C. A novel polysaccharide from *Acorus tatarinowii* protects against LPS-induced neuroinflammation and neurotoxicity by inhibiting TLR4-mediated MyD88/NF- κ B and PI3K/Akt signaling pathways. *Int J Biol Macromol* 2020;**163**:464–75.